



Contents lists available at ScienceDirect



Catalysis Today

journal homepage: www.elsevier.com/locate/cattod

Influence of co-feeds additive on the photo-epoxidation of propylene over V-Ti/MCM-41 photocatalyst

Van-Huy Nguyen^a, Shawn D. Lin^{a,*}, Jeffrey C.S. Wu^{b,**}, Hsunling Bai^c

^a Department of Chemical Engineering, National Taiwan University of Science and Technology, Taipei 10617, Taiwan

^b Department of Chemical Engineering, National Taiwan University, Taipei 10617, Taiwan

^c Institute of Environmental Engineering, National Chiao Tung University, Hsin Chu 300, Taiwan

ARTICLE INFO

Article history:

Received 30 November 2013

Received in revised form 10 June 2014

Accepted 26 June 2014

Available online xxx

Keywords:

Photo-epoxidation

co-Feed

H₂O

H₂

V-Ti/MCM-41 photocatalyst

ABSTRACT

In this work, the effects of co-feed species, namely, H₂O or H₂, on the photocatalytic epoxidation of propylene over V-Ti/MCM-41 are examined. A promoting effect on the C₃H₆ consumption rate is found under 0.6 kPa H₂O co-feed when the PO (propylene oxide) formation rate is not proportionally promoted, resulting a slightly decreased PO selectivity. With increasing H₂O concentration, the reaction activity decreases and this can be attributed to surface site blocking by excess H₂O. The presence of H₂O also increases the stability of photocatalyst during reaction. Similar observation of the enhanced C₃H₆ consumption rate and the improved stability is found when 5.6 kPa H₂ is used as co-feed. We found that the catalyst stability is improved when the AA (acetaldehyde) is increased. This suggests that AA accumulation on the catalyst surface may lead to surface fouling and the observed deactivation. The presence of H₂O or H₂ co-feed, which can lead to hydroxyl radical (OH•), may impose a shift in the production formation of photocatalytic reaction.

© 2014 Elsevier B.V. All rights reserved.

1. Introduction

For achieving a sustainable society, many efforts have been made to utilize clean energy sources, e.g., sunlight, in household applications and in industrial processes. Furthermore, using molecular oxygen as the oxidant of partial oxidation processes is a challenge concerning both economic and environmental issues in chemical industry. As a consequence, photocatalytic partial oxidation using molecular oxygen can be a key toward sustainable organic synthesis processes [1]. In this work, we discuss the photocatalytic synthesis of propylene oxide (PO), an industrially important epoxide chemical [2,3].

The direct gas phase photo-epoxidation of propylene to PO attracts much attention of both academic and industrial researchers [3]. We recently screened a series of photocatalysts for this photo-epoxidation reaction, including SiO₂, TiO₂, TS-1, V-Ti/MCM-41,

V₂O₅/SiO₂, Au/TiO₂ and Au/TS-1 [4,5]. Among these photocatalysts, bi-metal V-Ti oxides constructed within the framework of MCM-41 could achieve a high PO production rate.

For photocatalysis, in general, a pair of electrons (e⁻) and holes (h⁺) is formed on the catalyst surface during light-irradiated. The gas-phase O₂ can adsorb and transform to O₂⁻ when react with an electron. Its subsequent reaction with a positive hole can lead to surface atomic oxyradical which is considered as the active species for oxidation, e.g., the epoxidation of propylene [4].



In addition to oxyradical, hydroxyl radical (OH•) is also recognized as a key intermediate governing the products distribution of photo-epoxidation [6]. Hydroxyl radical is considered not only to prevent the recombination of electron-hole pairs but also can attack the reactants, resulting in enhancement of photo-activity [7]. Hence, we believed that the photo-epoxidation of propylene may be selectively altered by the presences of additional hydroxyl radical. Thus, the reaction pathway of this reaction can be elaborated. The inclusion of co-feeds such as H₂O, H₂O₂ or H₂ can generate hydroxyl radical (OH•) on photocatalysts. For example,

* Corresponding author at: National Taiwan University of Science and Technology, Chemical Engineering, 43, Keelung Rd., Sec.4, Taipei 106, Taiwan.
Tel.: +886 2 27376984; fax: +886 2 27376644.

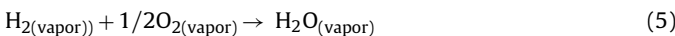
** Corresponding author at: National Taiwan University, Chemical Engineering, No. 1, Sec. 4, Roosevelt Road, Taipei 10617, Taiwan. Tel.: +886 2 23631994;
fax: +886 2 23623040.

E-mail addresses: sdlin@mail.ntust.edu.tw (S.D. Lin), [\(J.C.S. Wu\).](mailto:cswu@ntu.edu.tw)

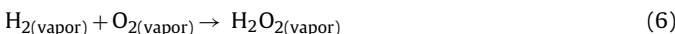
H_2O molecules could trap holes (h^+) to generate hydroxyl radical ($\text{OH}\bullet$) [8].



The reaction pathways for H_2 are still the subject of debate but both H_2O_2 and H_2O are possible intermediates. For example, H_2 oxidation to H_2O via the following reaction and subsequently leading to hydroxyl radicals.



Alternatively, it can react with O_2 to produce H_2O_2 intermediate



Then, H_2O_2 can be transformed into hydroxyl radical ($\text{OH}\bullet$) under light-irradiated [9], as that summarized below.



To date, only few studies have investigated the co-feeds effect on gas-phase photocatalytic reactions, and their effects are still a matter of debate. For example, Peral and Ollis reported that H_2O vapor inhibits the photo-degradation of acetone by using near-UV-irradiation over titanium dioxide (anatase) powder, but H_2O vapor has no influence on the degradation of 1-butanol [10]. H_2O vapor can enhance the acetic acid photo-decomposition on TiO_2 to increase the CH_4 formation rate [11]. Huang et al. carried out the catalytic toluene oxidation and observed a promotion by the presence of H_2O vapor [12]. Peral and Ollis reported that there is an optimum water vapor concentration in the photo-degradation of *m*-xylene, methanol and trichloroethylene [10]. Carneiro et al. recently proposed that humidity can play a role of “surface cleaning” to eliminate the accumulated deactivating species [13]. These results indicates that effect of H_2O co-feed on photocatalytic reaction can be complex and depends on the concentration of co-feed, but the influence of different types of co-feed is not known.

To the best of our knowledge, no systematic comparison on the presence of either H_2O or H_2 co-feed in photocatalytic epoxidation of propylene is reported yet. This study evaluates the effect of hydroxyl radical ($\text{OH}\bullet$), generating from the presence of H_2O or H_2 co-feeds, on photocatalytic epoxidation of propylene over V-Ti/MCM-41 photocatalyst. We had also tried to evaluate the effect of $\text{H}_2\text{O}-\text{H}_2\text{O}_2$ mixture. However, the preliminary results indicated H_2O_2 co-feed did not reveal significant enhancement in comparison to H_2O . How the presence of different co-feed may influence the activity and the stability of V-Ti/MCM-41 is illustrated. This may provide a strategy for optimization of photocatalytic activity by using co-feed species.

2. Experimental

2.1. Preparation of photocatalyst

The procedure of V-Ti/MCM-41 preparation was described in details previously [4]. First, aqueous solution of sodium metasilicate monohydrate (J.T. Baker) was combined with both titanium oxysulfate hydrate (Sigma-Aldrich) and vanadyl(IV) sulfate hydrate (17–23% V, Acros Organics), which were dissolved in 2 M H_2SO_4 (95–97%, Sigma-Aldrich), respectively. Next, cetyl trimethylammonium bromide (CTAB, 98%, Alfa Aesar) dissolved in 25 ml of deionized water was added slowly into the mixture. After stirring for 3 h, the gel mixture was transferred into autoclave and kept in an oven at 418 K for 36 h. After cooling to the room temperature, the resulting solid was washed and filtered with deionized water, dried at 383 K for 8 h, and then calcined at 823 K for 10 h.

2.2. Characterization of photocatalyst

The inductively coupled plasma-atomic emission spectra (ICP-AES, PerkinElmer Optima 2000) analysis was carried out to determine the chemical composition of the elements V, Ti and Si of V-Ti/MCM-41 photocatalyst. The specific surface area of catalyst was determined by the Brunauer–Emmett–Teller method (BET, ASAP2010 Micromeritics). The X-ray photoelectron spectroscopy (XPS, Thermo Scientific Theta Probe) was used to determine the oxidation states of the elements. Powder X-ray diffractometer (XRD, X-ray-M03XHF, Ultima IV) was used to verify the crystalline structure of the photocatalyst. The light absorption of photocatalyst was characterized by ultraviolet-visible light spectroscopy (UV-vis, Varian Cary-100). BaSO_4 was used as a standard reflection reference. Transmission electron microscope (TEM, Philips Tecnai F30 FEI) was performed to reveal the structure of mesoporous catalyst at an acceleration voltage of 200 kV.

2.3. Experimental setup

The catalyst (10 mg) was evenly spread in a photo-reactor (volume, ca. 0.55 cm³) equipped with a quartz window on top for light transmission. A one-way valve was installed between the reactor and the gas chromatograph to prevent flow out the catalyst under different pressure between the feed gases and sample injection. A gas mixture (at $\text{GHSV} = 6000 \text{ h}^{-1}$) of C_3H_6 (5.6 kPa) and O_2 (5.6 kPa) in N_2 was introduced into the photo-reactor. H_2 or H_2O was introduced into the gas mixture as co-feed. The H_2O vapor was carried by the reactant gas mixture passing through an impinger with H_2O liquid. The vapor concentration was controlled by the temperature of impinger. The values of H_2O vapor pressures were calculated based on the work of Manatt et al. [14]. After the reactant mixture became stable, UV-light was turned on using a mercury arc lamp (0.3 mW cm⁻², 320–500 nm). The reactor temperature was maintained at 323 K using a hot plate.

The effluent was analyzed periodically using in-line gas chromatograph (Young Lin, YL6100 GC) equipped with a flame ionization detector (FID) and a thermal conductivity detector (TCD). Carbon dioxide (CO_2) and oxygenated products (propylene oxide (PO), propionaldehyde (PA), acetone (AC), acetaldehyde (AA) and ethanol (ROH)) were separated using a Porapak-N packed column and analyzed by FID (except CO_2 via TCD). The lighter gases (H_2 , O_2 and N_2) were separated by a molecular sieve-5A capillary column and analyzed by TCD. The product formation rate, C_3H_6 consumption rate and the product selectivity are expressed as follows:

product formation rate

$$= \frac{\text{concentration of product detected on streamflow rate} \times \text{flow rate}}{\text{weight of photocatalyst}} \quad (9)$$

$$\text{C}_3\text{H}_6\text{consumption rate} = \sum \text{products formation rate} \quad (10)$$

$$\text{product selectivity} = \left(\frac{\text{product formation rate}}{\text{C}_3\text{H}_6\text{ consumption rate}} \right) \times 100\% \quad (11)$$

$$\text{H}_2\text{ conversion} = \left(\frac{\text{H}_2\text{ inlet}}{\text{H}_2\text{ outlet}} \right) \times 100\% \quad (12)$$

3. Results and discussion

3.1. Photocatalyst characterizations

The contents of Ti, V and Si of this V-Ti/MCM-41 catalyst were analyzed by ICP-AES and corresponded to 0.53, 0.05 and 46.29%,

respectively. The amount of V- and Ti-incorporated of MCM-41 is low, which is expected not to affect the MCM-41 lattice structure. XRD diffraction pattern (Fig. 1) exhibited an intense MCM-41 (1 0 0) peak and a band attributable to overlapped (1 1 0) and (2 0 0) peaks [15,16]. TEM image of V-Ti/MCM-41 (Fig. 2) revealed the uniform

ordered hexagonal structure, a distinctive feature of MCM-41, with a pore diameter of approximately 3 nm. The BET surface area of V-Ti/MCM-41 was approximately $790 \text{ m}^2 \text{ g}^{-1}$.

The UV-vis spectra of V-Ti/MCM-41 showed absorbance in the range of UV light ($\lambda < 400 \text{ nm}$) (Fig. 3). The absorbance can be attributed to that tetra-coordinated titanium and vanadium

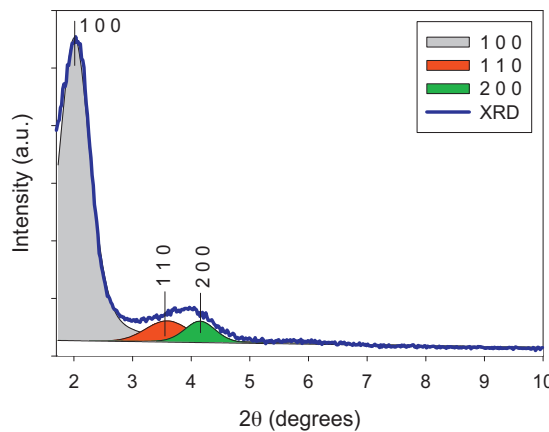


Fig. 1. Experimental and predicted element peaks of X-ray diffraction.

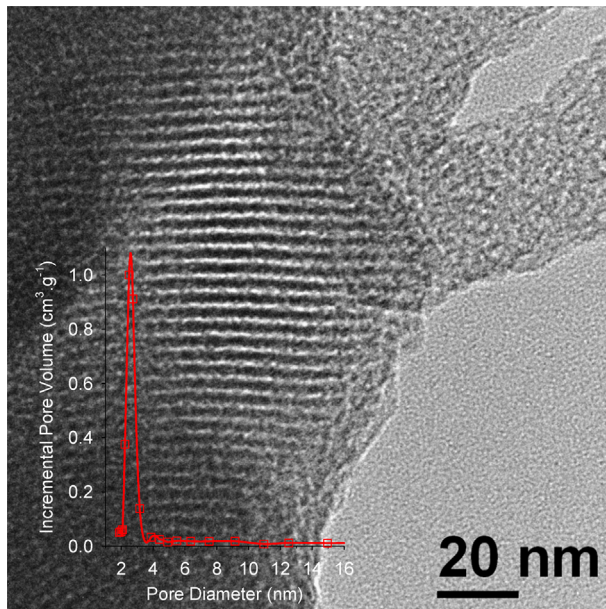


Fig. 2. TEM of V-Ti/MCM-41 photocatalyst, bar represents 20 nm.

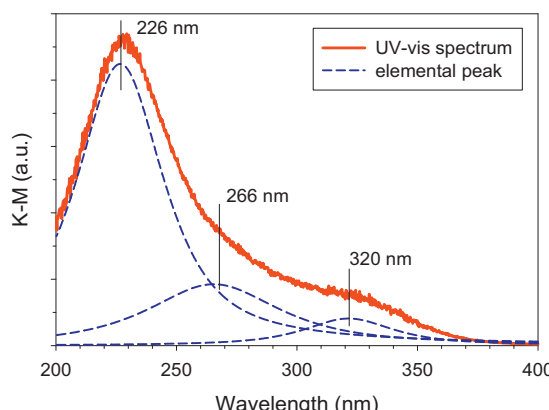


Fig. 3. Experimental and predicted element peaks of UV-vis spectroscopy.

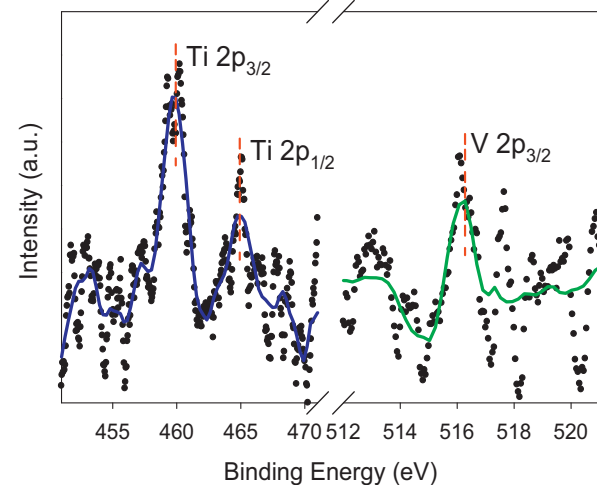


Fig. 4. XPS spectra: (a) titanium and (b) vanadium on V-Ti/MCM-41 photocatalyst.

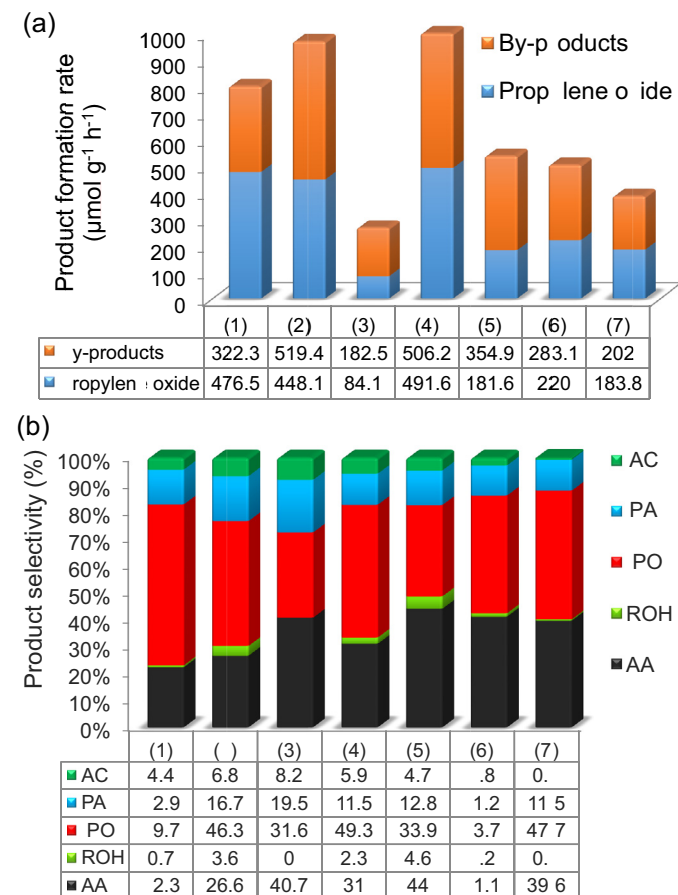


Fig. 5. (a) The propylene oxide (PO) and by-products formation rates and (b) the distribution of products in the photocatalytic epoxidation of propylene under different co-feed conditions: (1) without co-feed, (2) with 5.6 kPa H_2 , (3) with 0.6 kPa H_2O but without O_2 , (4) with 0.6 kPa H_2O , (5) with 3.2 kPa H_2O , (6) with 7.4 kPa H_2O , and (7) with 19.9 kPa H_2O . Abbreviations: propylene oxide (PO), propionaldehyde (PA), acetone (AC), acetaldehyde (AA) and ethanol (ROH).

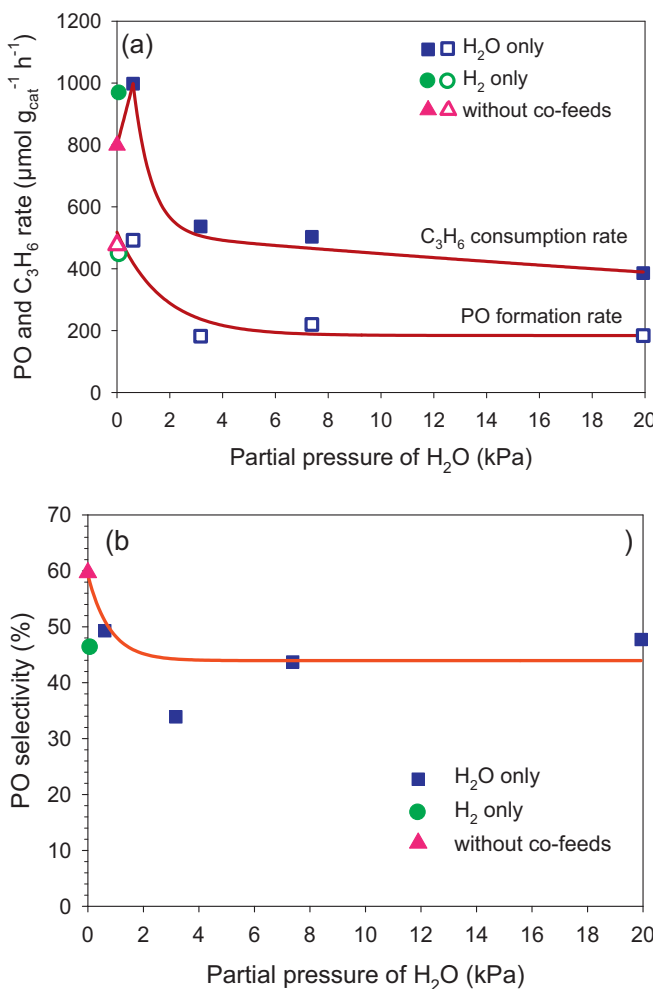


Fig. 6. Correlation between H₂O vapor pressures and (a) C₃H₆ consumption rate and PO formation rate, (b) PO selectivity.

species present in the +4 and +5 oxidation state, respectively, in the framework of MCM-41 support, with a strong band at 220–230 nm [17,18]. However, there may also exist hexa-coordinated Ti on extra-framework positions with a weak band at 266 nm [18]. A weaker band at 320 nm was observed and assigned to the charge transfer band of tetra-coordinated vanadium species [18]. XPS examinations showed the existence of well-defined peaks of Ti(2p) at 460 eV and 465.1 eV (Fig. 4). Its peak at 460 eV (Ti 2p_{3/2}) is usually assigned to titanium in tetrahedral coordination [19]. The binding energy of V 2p_{3/2} for V-Ti/MCM-41 is at 516.4 eV. Due to the little content of V and Ti, its XPS peak could not be observed clearly.

3.2. Photo-epoxidation of propylene

Typically, it needs to spend 2–3 h before reaching a steady-state conditions. There is no activity observed when either the photocatalyst or the UV illumination is absent. Evidently, the epoxidation over the V-Ti/MCM-41 catalyst is mainly photocatalytic epoxidation. The major products included PO, PA (propionaldehyde) and AA (acetaldehyde) while the minor products were AC (acetone) and ROH (ethanol).

The effects of co-feeds on the product formation rates are summarized in Fig. 5. During a reaction, the steady state also achieved with the standard errors in range of 1.0–9.7 μmol g_{cat}⁻¹ h⁻¹, 3.1–15.7 μmol g_{cat}⁻¹ h⁻¹ and 0.1–0.6% for PO formation rate, C₃H₆ consumption rate and PO selectivity, respectively. Among

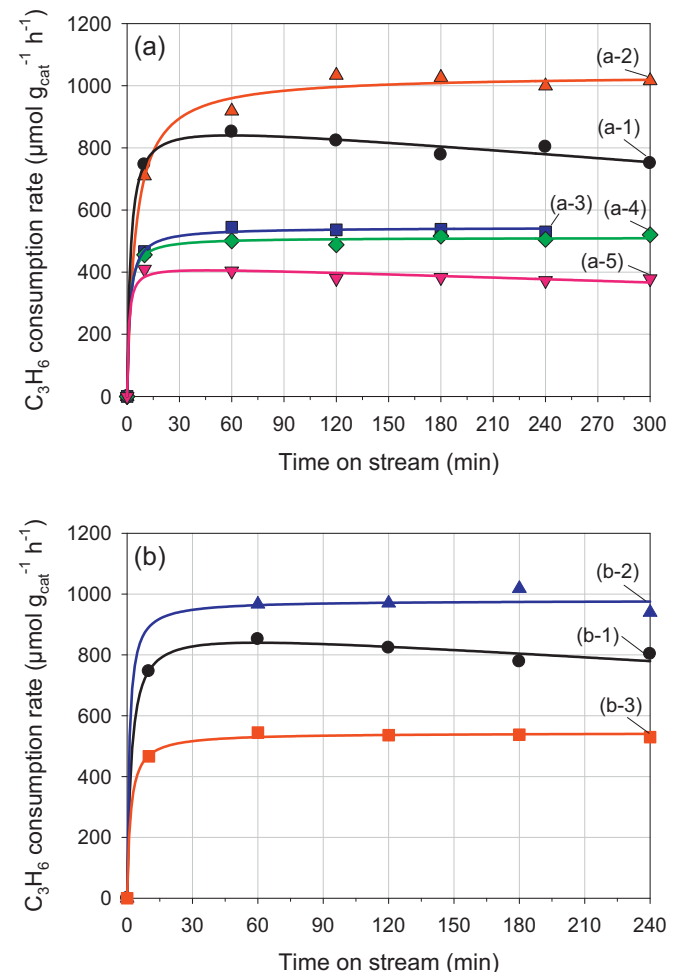


Fig. 7. The C₃H₆ consumption rate on-stream during reaction under different co-feed conditions: (a) H₂O: (a-1) 0 kPa, (a-2) 0.6 kPa, (a-3) 3.2 kPa, (a-4) 7.4 kPa and (a-5) 19.9 kPa; and (b) the direct comparison co-feed: (b-1) without co-feed, (b-2) with 5.6 kPa H₂, and (b-3) with 3.2 kPa H₂O.

the experimental conditions, run (4), in the presence of 0.6 kPa H₂O, yielded the highest C₃H₆ consumption rate of 997.8 μmol g_{cat}⁻¹ h⁻¹ and the highest PO formation rate of 491.6 μmol g_{cat}⁻¹ h⁻¹ (Fig. 5(a)). When excess H₂O is present, the photo-epoxidation activity decreased. For run (2) with 5.6 kPa H₂ co-feed, it also showed a higher C₃H₆ consumption rate of 967.5 μmol g_{cat}⁻¹ h⁻¹ than that of 798.8 μmol g_{cat}⁻¹ h⁻¹ when without co-feed but its PO formation rate was lower. The other runs with the different amount of co-feeding H₂O resulted in decreased activity performance. Fig. 5(b) displays the dependence of products selectivity on the co-feeds. Among the obtained results, 59.7% of PO selectivity in the absence of co-feed (run (1)) is the highest one. The decrease in PO selectivity when with co-feed is accompanied by an increase in the selectivity of AA.

Interestingly, with 0.6 kPa H₂O but in the absence of molecular oxygen (run (3)), PO was also formed but at a significantly lower selectivity than that with O₂ only (run (1)). In the previous study [4,20], we have mentioned that both titanium and vanadium exist in the tetrahedral coordination and those chemical oxidation species present in the +4 and +5 oxidation state, respectively, based on Ti and V K-edge XANES. Further study on XPS and UV-vis confirmed their environmental structure and chemical oxidation. On the whole, these species are able to form the corresponding charge-transfer excited states under UV-light irradiation [21].



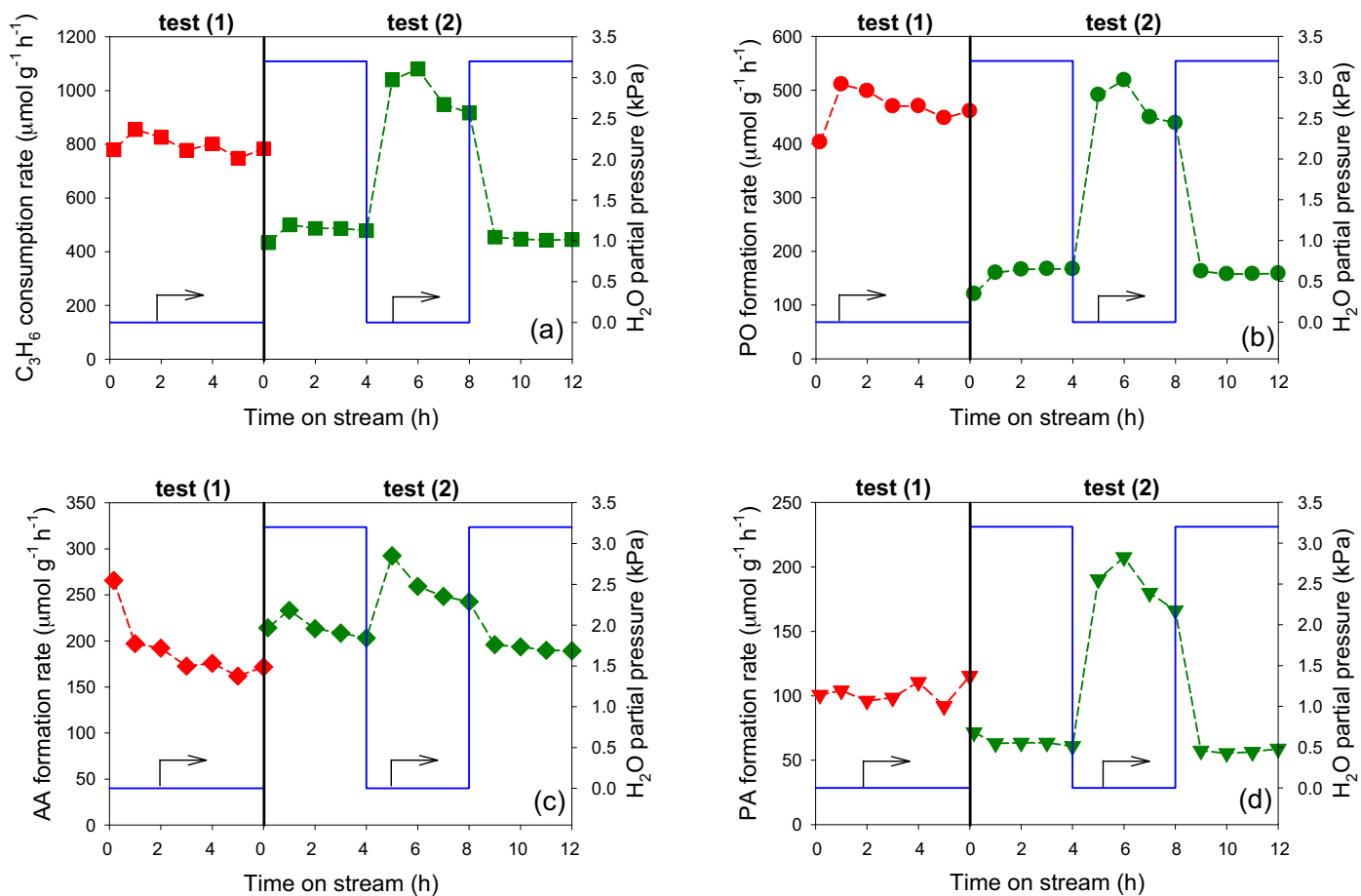
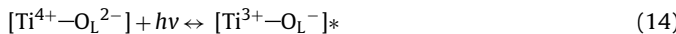


Fig. 8. The time profiles of reaction in either presence or absence of H_2O co-feed: (a) C_3H_6 consumption rate; and the formation rate of (b) propylene oxide (PO), (c) acetaldehyde (AA) and (d) propionaldehyde (PA).



Therefore, the lattice oxygen (O_L^{-}) species can react with C_3H_6 through C–C bond fission [22]. Then, under the presence of H_2O only, ($\text{O}_\text{L}^{-}-\text{CH}=\text{CH}_2$) will react with hydroxyl radical ($\text{OH}\cdot$) to form AA (H_3CCHO). Hence, the reaction between C_3H_6 in the presence of H_2O only without O_2 (run (3)) was still observed. However, its reaction pathway favors the formation of AA.

Fig. 6 shows the dependency of C_3H_6 consumption rate, PO formation rate, and PO selectivity on H_2O vapor pressure. Fig. 6(a) depicts that the C_3H_6 consumption rate is dramatically enhanced by co-feeding 0.6 kPa H_2O but it is depressed when the H_2O is at higher concentration. The enhancement is probably due to that holes can be scavenged by oxidizable species [23] generated from H_2O , in which causes a depression in electron–hole pairs recombination. In addition, the presence of hydroxyl radical ($\text{OH}\cdot$), which is generated from H_2O under light irradiation, can promote the photo-activity by attacking reactants directly [7]. On the other hand, other source of hydroxyl radical ($\text{OH}\cdot$) may derived from Si–OH is activated under photo-irradiation and would be consumed during reaction. Subsequently, the new ($\text{OH}\cdot$), which can be derived from the co-feeds, will take part in and implement the ones is consumed above. However, excess H_2O onto photocatalyst may be able to cause structural changes in surface band bending [8], resulting in favoring the recombination of photo-generated electron–hole pairs. The competition for the adsorptive sites between water and reactant molecules is another reason that can depress the photocatalytic activity [24]. The dual function in inhibition and promotion by co-feed observed in this study is consistent with the results of Peral

and Ollis [10] and Coronado et al. [7]. It is noted that the influence of co-feed in photocatalysis significantly depends on the species of reactants. Hence, it may have either inhibition or enhancement or both of two effects on photocatalytic reaction [7,25]. For the case using H_2 as co-feed, the conversion of H_2 is 1.6% during the reaction. Since we have mentioned that H_2O_2 showed less influence on the reaction than H_2O , the conversion of H_2 to H_2O would correspond to a $P_{\text{H}_2\text{O}}$ of 0.09 kPa which is addressed in Fig. 6(a). Its enhancement corresponds to the case using $P_{\text{H}_2\text{O}}$ of 0.6 kPa. Fig. 6(b) shows that no matter what co-feeds are, the selectivity to PO will drop to 45–50%. The competition for the adsorptive sites between co-feed, reactant and products molecules may be a reason.

To illustrate the influence of co-feed on the reaction stability, the time-dependent C_3H_6 consumption rate is compared (Fig. 7). A gradual deactivation is observed when in the absence of co-feed during reaction. We expect that the presence of co-feeds not only promote activity by preventing the recombination of electron–hole pairs but also enhance stability by eliminating the accumulated deactivating species. Fig. 7(a) shows that H_2O co-feed can suppress deactivation even though the C_3H_6 consumption rate was suppressed by excess H_2O . In recent work, Takeuchi et al. reported that products with a carbonyl group such as AA can easily adsorb on Ti^{4+} active sites [26]. Considering that both selectivity to AA and formation rate of AA were relatively enhanced by the presence of H_2O co-feed, this observation suggests that H_2O can suppress the accumulation of AA on the catalyst surface and consequently preventing the formation of larger and heavier species [27]. Only a slightly loss activity was observed for $P_{\text{H}_2\text{O}} = 19.9$ kPa (a–5). It may exist a balance between consumption and replenishment of hydroxyl

radical during reaction is strongly related to catalyst stability [25]. Hence, in the case of high partial pressure, excess hydroxyl radical generated may break the balance of consumption-replenishment, resulting in decreased stability. Fig. 7(b) confirms that either H₂O or H₂ co-feed can stabilize the catalyst activity.

Fig. 8 presents the transient photo-activity behavior when switching from the presence of 3.2 kPa H₂O co-feed to dry condition (test 2), where the time-on-stream behavior in the absence of H₂O co-feed is compared (test 1). The suppression of C₃H₆ consumption, PO formation, and PA formation rates by the 3.2 kPa H₂O is shown, which is the same as in case (a-3), Fig. 7. It was attributed to that excess H₂O covered the surface site. The nearly reversible rates observed from switching off 3.2 kPa H₂O and then back to its switch-on in test (2) supports that excess H₂O only physically blocking surface sites. In addition, all rates had a sudden increase when the 3.2 kPa was switched off. This behavior can be explained by that the gradual decrease in moisture content in the system resulting in the enhanced reaction rate, consistent with that shown in case (a-2) of Fig. 7 where small amount of H₂O enhanced activity. After consuming the adsorbed H₂O on the catalyst surface, the activity shows a tendency to drop back to that under dry conditions (test 1), Fig. 8. The AA formation was enhanced by the 3.2 kPa H₂O co-feed comparing to that under dry conditions, not like the other production formation rates. This and the enhanced stability observed in Fig. 7 suggests that AA accumulation on the surface is a possible reason of catalyst deactivation.

4. Conclusions

In summary, the effect of co-feed on the photo-epoxidation of propylene over V-Ti/MCM-41 was carefully investigated under UV-light irradiation 0.3 mW cm⁻² at 323 K. Their influence on photo-activity is quite complex and depends on H₂O partial pressure. Both activity and stability of the photo-epoxidation are promoted under 0.6 kPa H₂O. However, the photo-activity is not further promoted when H₂O pressure is over 0.6 kPa. The inclusion of 5.6 kPa H₂ can enhance the photo-activity and the catalyst stability. The promoting effects are accompanied by an increase in both selectivity and formation rate of AA. This suggests that co-feed can inhibit the AA accumulation on the catalyst surface which may lead to surface fouling, resulting in catalytic deactivation. The results of this study indicate that photocatalytic epoxidation of propylene

over V-Ti/MCM-41 is very sensitive to the presence/absence of H₂O and H₂ co-feeds.

Acknowledgement

The authors would like to acknowledge the financial support received from National Science Council Taiwan under contract NSC 99-2923-E-002-002-MY2.

References

- [1] S.-C. Chua, X. Xu, Z. Guo, Process Biochem. 47 (10) (2012) 1439–1451.
- [2] T.A. Nijhuis, M. Makkee, J.A. Moulijn, B.M. Weckhuysen, Ind. Eng. Chem. Res. 45 (10) (2006) 3447–3459.
- [3] H. Yoshida, Photocatalytic organic syntheses, in: M. Anpo, P.V. Kamat (Eds.), Environmentally Benign Photocatalysts, Springer, New York, NY, 2010, pp. 647–669.
- [4] V.-H. Nguyen, H.-Y. Chan, J.C.S. Wu, H. Bai, Chem. Eng. J. 179 (0) (2012) 285–294.
- [5] V.-H. Nguyen, H.-Y. Chan, J. Wu, J. Chem. Sci. 125 (4) (2013) 859–867.
- [6] V.-H. Nguyen, J.C.S. Wu, H. Bai, Catal. Commun. 33 (0) (2013) 57–60.
- [7] J.M. Coronado, M.E. Zorn, I. Tejedor-Tejedor, M.A. Anderson, Appl. Catal., B: Environ. 43 (4) (2003) 329–344.
- [8] M. Anpo, K. Chiba, M. Tomonari, S. Coluccia, M. Che, M.A. Fox, Bull. Chem. Soc. Jpn. 64 (2) (1991) 543–551.
- [9] R.S. Thakur, R. Chaudhary, C. Singh, Renewable Sustainable Energy 2 (4) (2010) 1–37, p. 042701.
- [10] J. Peral, D.F. Ollis, J. Catal. 136 (2) (1992) 554–565.
- [11] D.S. Muggli, J.L. Falconer, J. Catal. 187 (1) (1999) 230–237.
- [12] H. Huang, D.Y.C. Leung, G. Li, M.K.H. Leung, X. Fu, Catal. Today 175 (1) (2011) 310–315.
- [13] J.T. Carneiro, C.-C. Yang, J.A. Moulijn, G. Mul, J. Catal. 277 (2) (2011) 129–133.
- [14] S.L. Manatt, M.R.R. Manatt, Chem. Eur. J. 10 (24) (2004) 6540–6557.
- [15] Y. Hu, N. Wada, K. Tsujimaru, M. Anpo, Catal. Today 120 (2) (2007) 139–144.
- [16] D. Marino, N.G. Gallegos, J.F. Bengoa, A.M. Alvarez, M.V. Cagnoli, S.G. Casuscelli, E.R. Herrero, S.G. Marchetti, Catal. Today 133–135 (0) (2008) 632–638.
- [17] W.A. Carvalho, P.B. Varaldo, M. Wallau, U. Schuchardt, Zeolites 18 (5–6) (1997) 408–416.
- [18] S.C. Laha, R. Kumar, Microporous Mesoporous Mater. 53 (1–3) (2002) 163–177.
- [19] M.C. Capel-Sánchez, J.M. Campos-Martín, J.L.G. Fierro, M.P. de Frutos, A.P. Polo, Chem. Commun. (10) (2000) 855–856.
- [20] V.-H. Nguyen, S.D. Lin, J.C.-S. Wu, H. Bai, J. Beilstein, Nanotechnology 5 (2014) 566–576.
- [21] M. Anpo, T.-H. Kim, M. Matsuoka, Catal. Today 142 (3–4) (2009) 114–124.
- [22] C. Murata, H. Yoshida, J. Kumagai, T. Hattori, J. Phys. Chem. B 107 (18) (2003) 4364–4373.
- [23] I. Izumi, W.W. Dunn, K.O. Wilbourn, F.-R.F. Fan, A.J. Bard, J. Phys. Chem. 84 (24) (1980) 3207–3210.
- [24] M.L. Sauer, D.F. Ollis, J. Catal. 149 (1) (1994) 81–91.
- [25] S.B. Kim, S.C. Hong, Appl. Catal., B: Environ. 35 (4) (2002) 305–315.
- [26] M. Takeuchi, J. Deguchi, S. Sakai, M. Anpo, Appl. Catal., B: Environ. 96 (1–2) (2010) 218–223.
- [27] S. Luo, J.L. Falconer, J. Catal. 185 (2) (1999) 393–407.